energies

MDPI

Article

Continuous Biohydrogen Production from Molasses via Dark Fermentation

Zheng-Ting Luan [1] and Chiu-Yue Lin [1,2,*]

[1] Department of Environmental Science and Engineering, Feng Chia University, Taichung 407102, Taiwan; yo349882@gmail.com
[2] Green Energy and Biotechnology Industry Research Center, Feng Chia University, Taichung 407102, Taiwan
* Correspondence: cylin@fcu.edu.tw

Abstract

Dark fermentation is commonly used for producing biohydrogen as a green hydrogen, which can be used as an alternative to fossil fuels. Pilot-scale studies on continuous biohydrogen production from molasses are still limited. In this study, a 60 L pilot-scale up-flow anaerobic sludge bed (UASB) dark fermentation system was operated continuously for biohydrogen production from molasses. The reactor achieved an average hydrogen production rate of 3.64 L H_2/L-d. Attention was paid to evaluating total sugar, rather than COD alone, as a more appropriate process indicator for substrate conversion and hydrogen production performance. In addition, metabolic pathway characteristics and microbial community structure were examined. The results provide useful pilot-scale operational data for the implementation of fermentative biohydrogen production technology.

Keywords: butyrate/acetate concentration ratio; fermentative biohydrogen production; microbial community structure; molasses substrate; organic loading indicator; pilot-scale bioreactor; total sugar concentration

1. Introduction

Based on net-zero emissions policy, hydrogen is considered one of the alternative fuels of the future because it is a sustainable and efficient energy source. Hydrogen has a higher energy content per unit mass compared to other fuels and produces virtually no greenhouse gases in combustion usage. However, more than 96% of the H2 produced worldwide is mainly obtained from the petrochemical industry, which involves environmentally unfriendly generation [1]. Therefore, searching for sustainable and environmentally friendly generation methods is desirable.

Anaerobic digestion is widely applied due to its capability to simultaneously stabilize organic matter and generate biogas (mainly methane, in percentages of 50–75%), supported by mature engineering practices and high adaptability across diverse operational contexts [2,3]. Another form of digestion that is widely applied is dark fermentation (DF), an anaerobic process converting organics into biogas (mainly hydrogen, in percentages of 30–60%) through acidification or hydrogenesis, which generates volatile fatty acids (VFAs) [2,4,5]. The biological production of H_2 using the DF process is now widely recognized, since this method does not require the use of fossil fuels or electricity; this kind of hydrogen is generally called biohydrogen [1,6,7], though some works have reported that biohydrogen might be produced from reforming biogas-based methane [8].

Check for updates

Academic Editor: Alberto Pettinau

Received: 17 March 2026
Revised: 14 April 2026
Accepted: 20 April 2026
Published: 22 April 2026

Copyright: © 2026 by the authors. Licensee MDPI, Basel, Switzerland. This article is an open access article distributed under the terms and conditions of the Creative Commons Attribution (CC BY) license.

There are many organic wastes used for producing renewable biohydrogen, such as agricultural wastes [7], food wastes [9], wastewaters [6], and molasses [10–12]. In Taiwan, Taiwan Sugar Corporation is the biggest company that produces molasses; it explores the value-added bioresources, including biogases, produced from it through DF [13]. Although pilot-scale and full-scale studies on biohydrogen production from molasses have been reported [10,12], there are still relatively few reports focusing on the use of pilot-scale bioreactors, especially for different reactor configurations, because of the complicated biochemical reactions involved and the need for a large amount of feedstock [14]. However, it is important to have pilot-scale knowledge for commercializing biohydrogen production technology [15]. The use of pilot-scale bioreactors would be helpful in providing effective engineering data in this field. Therefore, a pilot-scale UASB system could be used to obtain useful information for implementing molasses-based biohydrogen production technology.

For the performance evaluation of biohydrogen production, most existing studies use chemical oxygen demand (COD) removal or express hydrogen yields on a COD-based basis. However, during dark fermentative hydrogen production, most of the influent organic carbon is converted into soluble intermediate metabolites rather than being fully mineralized. In contrast, using fermentable carbohydrates (total sugars) as the reference basis more accurately reflects the true substrate availability for hydrogen-producing microorganisms and facilitates a more rational comparison between observed hydrogen production and theoretical conversion efficiencies.

Based on the above considerations, this study aimed to evaluate the continuous performance of a 60 L pilot-scale UASB dark fermentation system for biohydrogen production from molasses. In addition to reporting reactor operational data, this study examined whether total sugar could serve as a more appropriate process indicator than COD alone for evaluating hydrogen production performance. During continuous operation, hydrogen production rate (HPR), hydrogen yield (HY), substrate removal behavior, VFA profiles, and shifts in microbial community structure were systematically monitored.

2. Materials and Methods

2.1. Seed Sludge and Substrate Wastewater

The inoculum was a mixed anaerobic hydrogen-producing consortium enriched in our laboratory, with *Clostridium* spp. as the dominant taxa. Previous studies have identified *Clostridium* as key functional microorganisms in dark fermentative hydrogen production, and their relative abundance has been shown to be significantly and positively correlated with biohydrogen production performance [16]. Given that sugarcane molasses was used as the primary feedstock in subsequent continuous biohydrogen production operation, the consortium was pre-acclimated and enriched using sucrose as the sole carbon source prior to reactor inoculation, to enhance adaptation to high-carbon molasses substrate and hydrogenic activity.

The inoculum used for startup was taken from the effluent of a laboratory-scale continuous anaerobic hydrogen-producing reactor, which had been cultivated on sucrose at a total sugar concentration of 20 g/L. For startup of the 60 L pilot-scale reactor, 10 L of inoculum effluent was mixed with 50 L of molasses-based substrate. The volatile solid (VS) concentrations of the inoculum and substrate were 10.45 ± 0.05 and 10.28 ± 0.12 g/L, respectively, corresponding to an inoculum-to-substrate ratio (ISR) of 0.20 g $VS_{inoculum}$/g $VS_{substrate}$. This ISR falls within a range reported to be suitable for fermentative biohydrogen production systems.

The substrate was a mixture of sugarcane molasses and bamboo hydrolysate with a ratio of 99:1 (%, *v*/*v*). Sugarcane molasses was collected from TaiSugar Dalin Refinery, one of Taiwan Sugar Corporation's companies located in central Taiwan. The raw sugarcane

molasses had a total sugar concentration of 562 g/L and a COD of 794 g/L, whereas the raw acid hydrolysate contained a total sugar concentration of 29.1 g/L and a COD of 37.3 g/L. Sugarcane molasses is a carbon-rich and nitrogen-deficient organic product. When directly used as a fermentation substrate, nutrient limitations can constrain microbial growth and metabolic activity, thereby reducing hydrogen production efficiency or cause process instability [17]. Accordingly, urea (CH_4N_2O) was supplemented in an amount of 2 g/L to adjust the carbon/nitrogen ratio of the feedstock and to satisfy the nitrogen requirements of the hydrogenic consortium.

2.2. Reactor, Operation, and Analytical Methods

An up-flow anaerobic sludge blanket (UASB) reactor constructed of stainless steel was employed, with a working volume of 60 L (internal diameter 20.4 cm, height 184 cm). The reactor had a vertical cylindrical configuration. The substrate was introduced from the reactor bottom and passed upward through the sludge bed, while a gas–liquid outlet at the top directed the mixed stream to an external gas–liquid separator. For startup, the reactor was inoculated with 10 L of acclimated hydrogen-producing effluent and mixed with 50 L of molasses-based substrate. The substrate was first homogenized in an external mixing tank and then delivered to the reactor bottom by a feeding pump. The hydraulic retention time (HRT) was maintained at 8 h, corresponding to an average equivalent flow rate of 7.5 L/h.

The operating temperature and pH were maintained at 37 °C and 6.0 ± 0.5, respectively. Temperature was controlled by indirect heat exchange using heated water circulated through an internal spiral metal coil. An internal recirculation system was used to improve liquid mixing and mass transfer. Temperature, pH, and oxidation-reduction potential (ORP) were monitored online through sensors installed in the recirculation line. The pH was controlled by feedback dosing of 6 N NaOH into the recirculation line when necessary.

Steady-state conditions were defined as the period during which the key performance indicators, including HPR and hydrogen content, remained relatively stable, with variations within ±15%. Based on this criterion, days 19–28 were identified as the steady-state period, and the average HPR, HY, COD removal, and sugar removal values reported in this study were calculated from this period. Hydrogen yield was expressed on two different bases in this study. COD-based HY was calculated as the volume of hydrogen produced per unit of net COD removed, whereas sugar-based HY was calculated as the volume of hydrogen produced per unit of total sugar consumed.

Biogas production was measured using a wet-type gas flow meter (Ritter TG1/5). Gas composition was analyzed using a gas chromatograph equipped with a thermal conductivity detector (China Chromatograph Personal-GC1000, China Chromatography Co., Ltd., New Taipei City, Taiwan). Argon was used as carrier gas, and separation was achieved using an Agilent PoraPak Q column (80/100 mesh, 3 m × 1/8-inch, 2 mm i.d.; Agilent Technologies, Santa Clara, CA, USA). The injector temperature was 140 °C, while the detector and column temperatures were maintained at 110 °C and 30 °C, respectively.

Liquid-phase characteristics were analyzed as follows. Total solids, volatile solids, and COD were determined in accordance with Standard Methods [18]. Hexose concentrations were quantified using the anthrone–sulfuric acid method [19]. Ethanol and VFAs were analyzed using a gas chromatograph (SHIMADZU GC-2014, Shimadzu Corporation, Kyoto, Japan) equipped with an ID-SOLGEL-WAX capillary column, with the column temperature set at 250 °C, the injector temperature set at 250 °C, and nitrogen as the carrier gas.

Gas-phase parameters, including HPR, hydrogen content, pH, and ORP, were obtained as single measurements at each sampling time. Therefore, the values shown in Figure 1 are presented without error bars. In contrast, liquid-phase parameters, including COD,

total sugar, and soluble metabolites, were analyzed in triplicate, and the values shown in Figure 2 are presented as the mean ± standard deviation.

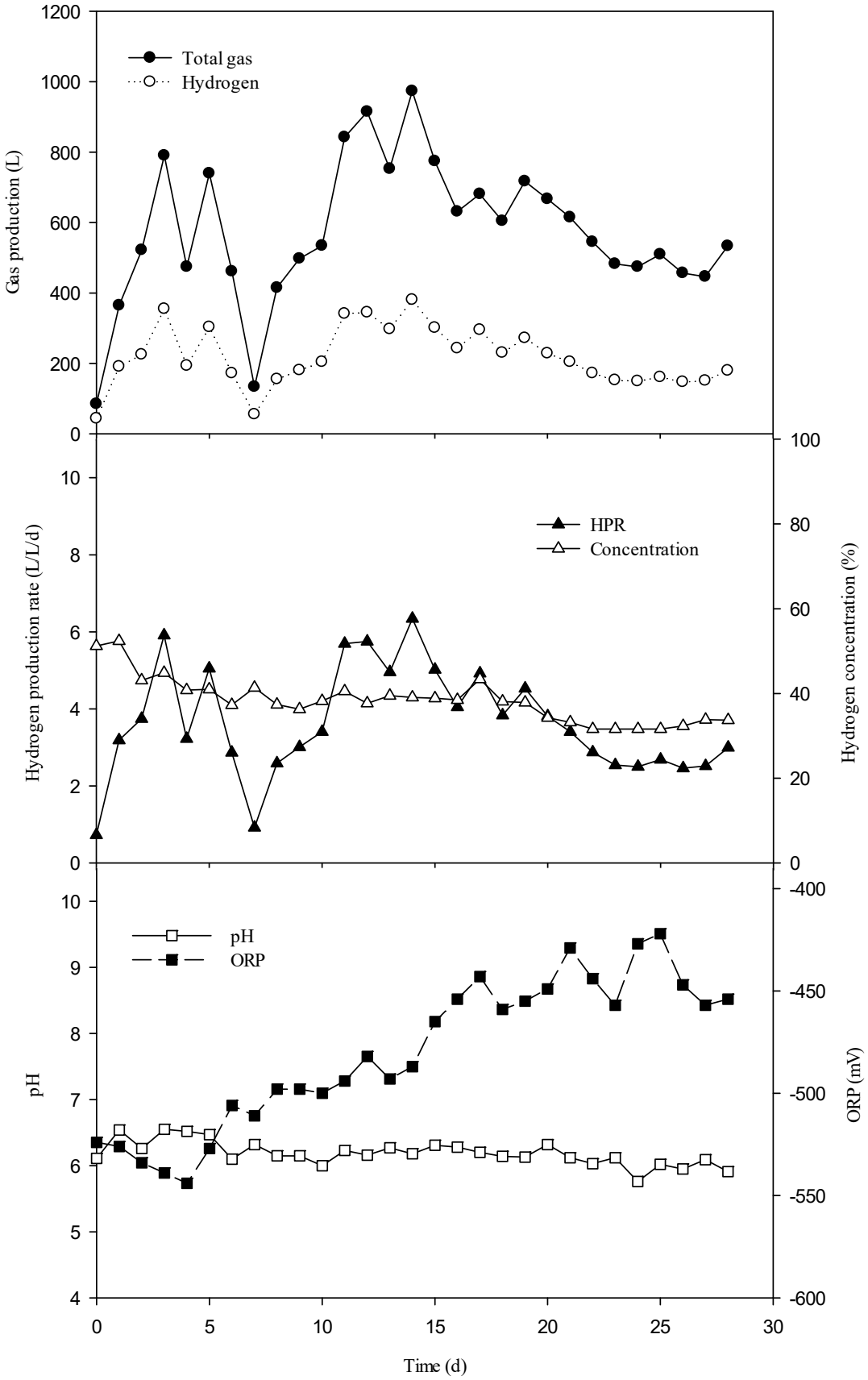


Figure 1. Daily variations in pH, ORP, hydrogen production rate, and hydrogen concentration.

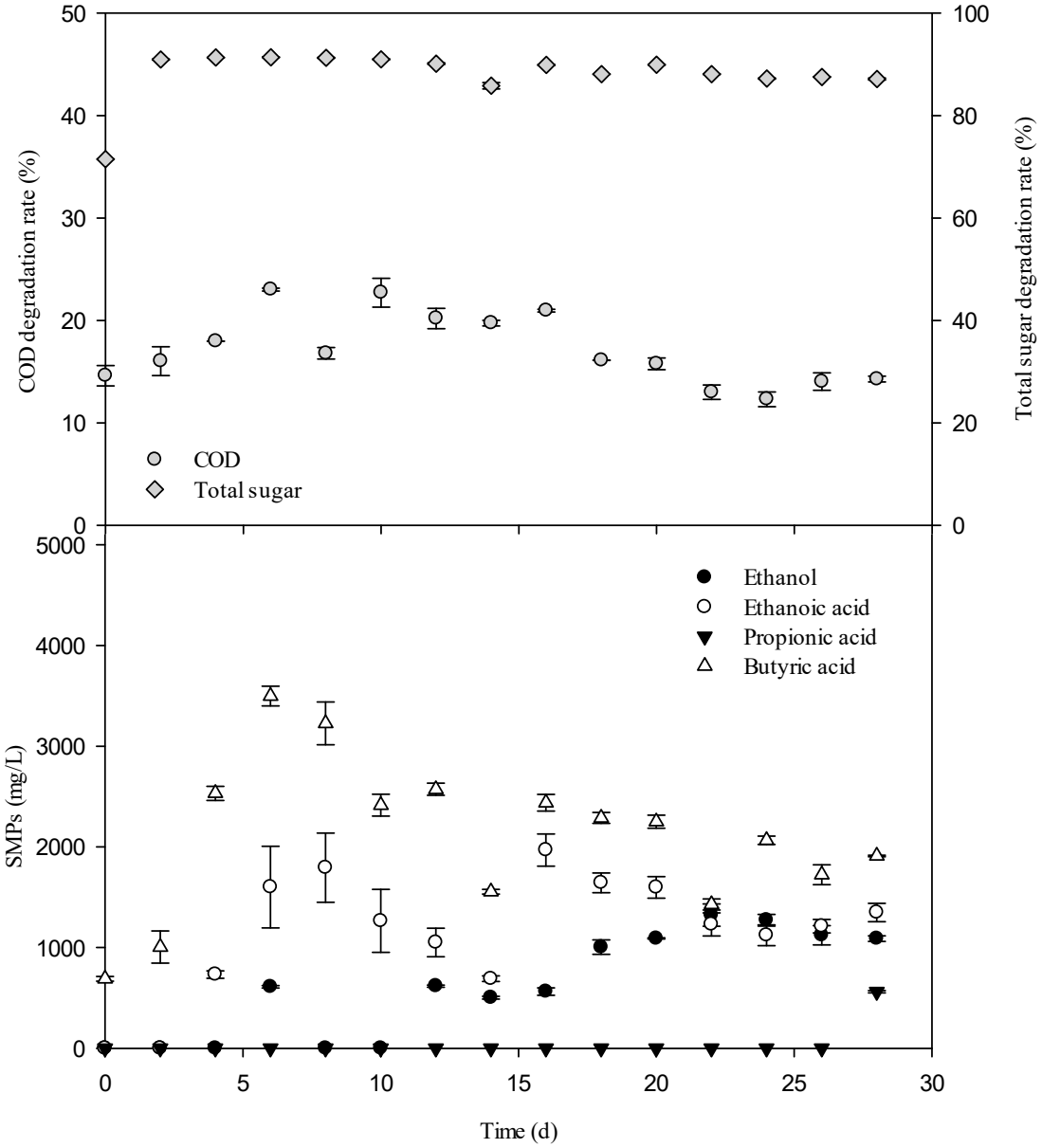


Figure 2. Daily variations in COD and total sugar removal efficiencies and soluble metabolite product (SMP) concentrations.

Microbial community analysis was performed by a commercial sequencing service provider. Genomic deoxyribonucleic acid was extracted using the DNeasy PowerSoil Kit (QIAGEN GmbH, Hilden, Germany). The bacterial 16S rRNA gene was amplified by barcoding polymerase chain reaction (PCR) using a barcode-tagged 341F forward primer and the 805R reverse primer (Tri-i Biotech, Inc., New Taipei City, Taiwan). The PCR products were purified, pooled, gel-extracted for the target band, and subsequently prepared for sequencing. Amplicon sequencing was conducted on an Illumina MiSeq platform (Illumina, Inc., San Diego, CA, USA) using 2 × 301 bp paired-end sequencing. Raw reads were quality-filtered, merged, and processed to generate effective reads. Amplicon sequence variants (ASVs) were inferred using DADA2 implemented in QIIME2 (v2020.8), and taxonomic assignment was performed against the SILVA database (release 138). Taxonomy profiling was conducted using QIIME2 and Krona, while alpha-diversity and rarefaction analyses were performed using QIIME v1.8.0.

3. Results and Discussion

3.1. Feedstock Characteristics and Dosing Strategy

The stable operation of a DF system primarily depends on the use of an appropriate feeding strategy. Conventional anaerobic digestion is largely designed for wastewater treatment, where influent loading control is typically based on COD [2,20,21]. However, the key functional microorganisms in hydrogenesis (e.g., *Clostridium* spp.) predominantly metabolize readily degradable carbohydrates. When feeding strategies are formulated solely on a COD basis, substrates with high COD concentrations but fermentable sugars may only be present in a low fraction, thereby limiting hydrogen production performance and constraining reaction kinetics. Moreover, biohydrogen production could generate many VFAs that are COD-related components [22]. In addition, there are some COD components in molasses, particularly complex polysaccharides, melanoidins, and high concentrations of VFAs or nitrogenous compounds, that are difficult to convert into biohydrogen [23,24]. While sugary fractions convert easily, these recalcitrant compounds often require long HRT or pre-treatment to break down. All of these factors create the need to consider another proper feeding indicator.

From the perspective of bioenergy recovery performance assessment, using total sugar concentration as the feeding basis is physiologically more consistent than COD and more accurately reflects the actual substrate availability required by hydrogen-producing microorganisms. Accordingly, this study adopted a total sugar concentration of 20 g/L as the influent setpoint for the reactor because some reports show that this concentration could result in peak biohydrogen production [11,25]. This strategy was intended to provide tighter control over substrate conversion rates, fermentation pathway distribution, and VFA production profiles, thereby improving the reproducibility of operating conditions and gas production performance at the pilot scale.

3.2. Biohydrogen Production Performance

3.2.1. HPR and HY

In fermentative biohydrogen production, carbohydrates are rapidly converted into VFAs and hydrogen. Figure 1 plots daily variations in pH, oxidation reduction potential (ORP), HPR, and hydrogen concentration in the produced gas. pH was an operation parameter and was controlled at around 6. ORP values ranged from −430 mV to −510 mV, normal values favoring fermentative biohydrogen production. These highly reducing, anaerobic conditions are essential for maximizing hydrogenase activity, favoring Clostridium growth, and suppressing methanogenic activity [26,27].

During steady-state operation, the HPR reached an average of 3.64 L H_2/L-d, which is within the upper range of values reported for molasses-based systems [10,12,28]. However, direct comparison among studies should be made cautiously because of differences in reactor configuration, scale, operating conditions, and substrate characteristics. When calculated on a $COD_{removed}$ basis, the HY averaged as high as 0.26 L H_2/g $COD_{removed}$. However, because most of the influent COD was converted into VFAs and retained in the liquid phase, using $COD_{removed}$ as the sole reference tends to inflate the apparent energy recovery and introduces interpretive bias [29]. When recalculated based on fermentable sugar consumption (total $sugar_{removed}$), the average HY was 0.07 L H_2/g, which more accurately reflects the true conversion efficiency and enables a meaningful comparison with theoretical yields, thereby confirming the characteristic of dark fermentative hydrogen production as a high-rate but low-efficiency process. This observation is consistent with previous dark fermentation studies, which have shown that hydrogen yields based on fermentable sugar removal would be better at reflecting actual metabolic conversion efficiency than COD-based conventional expression [30]. Note that having a complete mass

balance is helpful in elucidating the exact significances of using total sugar concentration as a better indicator in operating molasses-based biohydrogen production. This mass balance (such as COD balance) would require additional quantifications of all soluble metabolites, gaseous carbon products, and biomass concentrations.

3.2.2. Metabolites

In DF, acidogenesis would generate hydrogen and carbon dioxide as gaseous products and alcohols and VFAs as liquid metabolites [2,22]. Figure 2 plots daily concentration variations in COD and metabolites of ethanol, acetic, propionic, butyric and valeric acids. For the metabolites, their concentrations showed a trend of increase and then decrease, which agrees with many reports of laboratory-scale DF.

Substrate conversion results indicated that, during steady-state operation, the reactor achieved COD and total sugar removal efficiencies of approximately 13.4% and 88%, respectively, reflecting a fermentative hydrogen production pattern characterized by high sugar conversion but low COD removal. This outcome demonstrates that influent carbohydrates were effectively transformed into soluble intermediates, while most organic carbon remained in the liquid phase as VFAs and had not yet undergone complete mineralization. Accordingly, these findings further confirm that evaluating reactor performance solely on a COD removal basis underestimates its functional role in carbon flux transformation and pretreatment.

To provide additional quantitative support for this interpretation, the major soluble metabolites observed at steady-state conditions were converted into COD equivalents. Based on the measured concentrations, butyrate (2300 mg/L), acetate (1300 mg/L), and ethanol (1150 mg/L) corresponded to approximately 4.18, 1.39, and 2.4 g COD/L, respectively, giving a subtotal of 7.97 g COD/L retained in the liquid phase. In addition, based on the influent total sugar setpoint of 20 g/L and a sugar removal efficiency of 88%, the removed sugar was estimated to be 17.6 g/L, whereas COD removal was only 13.4%. These results indicate that a substantial fraction of substrate conversion was directed toward soluble intermediates rather than net COD removal. Therefore, HY based on sugar removal more directly reflects fermentable substrate-to-hydrogen conversion than HY based only on $COD_{removed}$. Nevertheless, this should still be regarded as a partial COD/carbon balance, and a complete balance would be needed for more rigorous validation.

During steady-state conditions, butyric acid was observed as the major VFA followed by acetic acid and ethanol, with concentrations of around 2300, 1300, and 1150 mg/L, respectively. The current work used the concentration and component variations in some metabolites to elucidate the performance of DF [2,31]. The high butyric acid concentration of 2300 mg/L indicates that the biohydrogen production was butyrate-type fermentation. This fermentation type is highly relevant for waste-to-energy applications. Moreover, the concentration ratio of butyric acid to acetic acid reached 1.8. Reports show that high concentrations of butyric acid to acetic acid would result in high biohydrogen production potential [31,32]. This also indicates the successful performance of the pilot-scale biohydrogen production bioreactor.

Note that ethanol reached a value of 1150 mg/L during the steady-state period, although it was not detected in the raw molasses feed (Figure 2). Recently, Ren et al. [12] reported an ethanol-type fermentation pathway in full-scale CSTR biohydrogen production from molasses. Therefore, the ethanol accumulation observed in the present study may suggest that part of the carbon flux and reducing equivalents was diverted to an ethanol-producing pathway, rather than being fully directed to hydrogen production. On the other hand, previous studies have also reported that ethanol may inhibit fermentative hydrogen production under certain conditions [10,33].

In the present system, 1150 mg/L ethanol corresponds to approximately 25 mmol/L. Based on the batch data reported by Wang et al. [33], this concentration would be expected to cause only mild inhibition, with estimated reductions of about 1.5–2% in substrate degradation efficiency, 11–13% in hydrogen yield, and 5.4% in hydrogen production rate. Therefore, ethanol in the present system may represent both a competing metabolic product and a possible secondary inhibitory factor, rather than a major inhibitor.

3.3. Microbial Community Structure

The microbial community analysis is shown in Figure 3. Marked changes in the microbial community in the reactor were observed before and after continuous operation, reflecting the selective effects imposed by operating conditions and substrate acclimation. At the phylum level, *Firmicutes* remained the dominant phylum both before and after acclimation, indicating that the operational environment of this system—characterized by high organic loading, mildly acidic conditions, and sugar-rich substrates—favored the enrichment of this phylum. *Firmicutes*, particularly genera like *Clostridium* and *Bacillus*, are the dominant bacteria driving biohydrogen production through anaerobic dark fermentation, and they use Fe-dependent hydrogenase enzymes to convert organics [34,35]. At the class level, *Clostridia* accounted for approximately 55% of the total community prior to continuous operation and slightly decreased to 46% after acclimation. This shift suggests that community changes were mainly attributable to an internal structural shift rather than simple biomass expansion or the elimination of key functional groups.

To further elucidate the internal shifts within the *Clostridia* lineage, the *Clostridia* subgroup was extracted from the overall community for comparative analysis (Figure 3, lower panels). Prior to continuous operation, the internal structure of *Clostridia* exhibited a pronounced single-dominant-taxon pattern, with *C. butyricum* accounting for approximately 70% of the *Clostridia* population, indicating a highly concentrated functional structure in the initial inoculum. After acclimation, the *Clostridia* community transitioned toward a more diversified and coexisting consortium structure. In addition to *C. butyricum*, the relative abundances of *C. pasteurianum*, *C. sensu stricto 1*, and multiple uncultured/unclassified clostridial taxa increased, resulting in a distribution of hydrogenic potential across multiple functional units.

Moreover, at the whole-community level, the relative abundance of *Bacilli* (e.g., *Leuconostoc mesenteroides*) increased markedly after acclimation, indicating that certain acid-tolerant or fast sugar-metabolizing taxa can coexist under conditions of high organic loading and acidification. These taxa may interact with clostridial populations through the production of intermediate metabolites (e.g., *lactate*), thereby indirectly influencing substrate fluxes and hydrogenic metabolic pathways [36]. Notably, the proportion of unclassified taxa with unclear functional roles decreased after acclimation, suggesting that the applied operation conditions exerted a selective pressure against non-target microorganisms.

Overall, although the relative abundance of *Clostridia* within the total community decreased from 55% to 46%, its internal structure shifted from a single-dominant-taxon one to a functionally cooperative, multi-taxon consortium. This acclimation-driven microbial structure indicates the development of functional partitioning and redundancy within the reactor. Such community restructuring is expected to enhance system resilience to load fluctuations and operational perturbations, reduce the risk of process instability caused by the environmental sensitivity of a single keystone species, and thereby confer practical advantages for continuous operation and engineering-scale implementation.

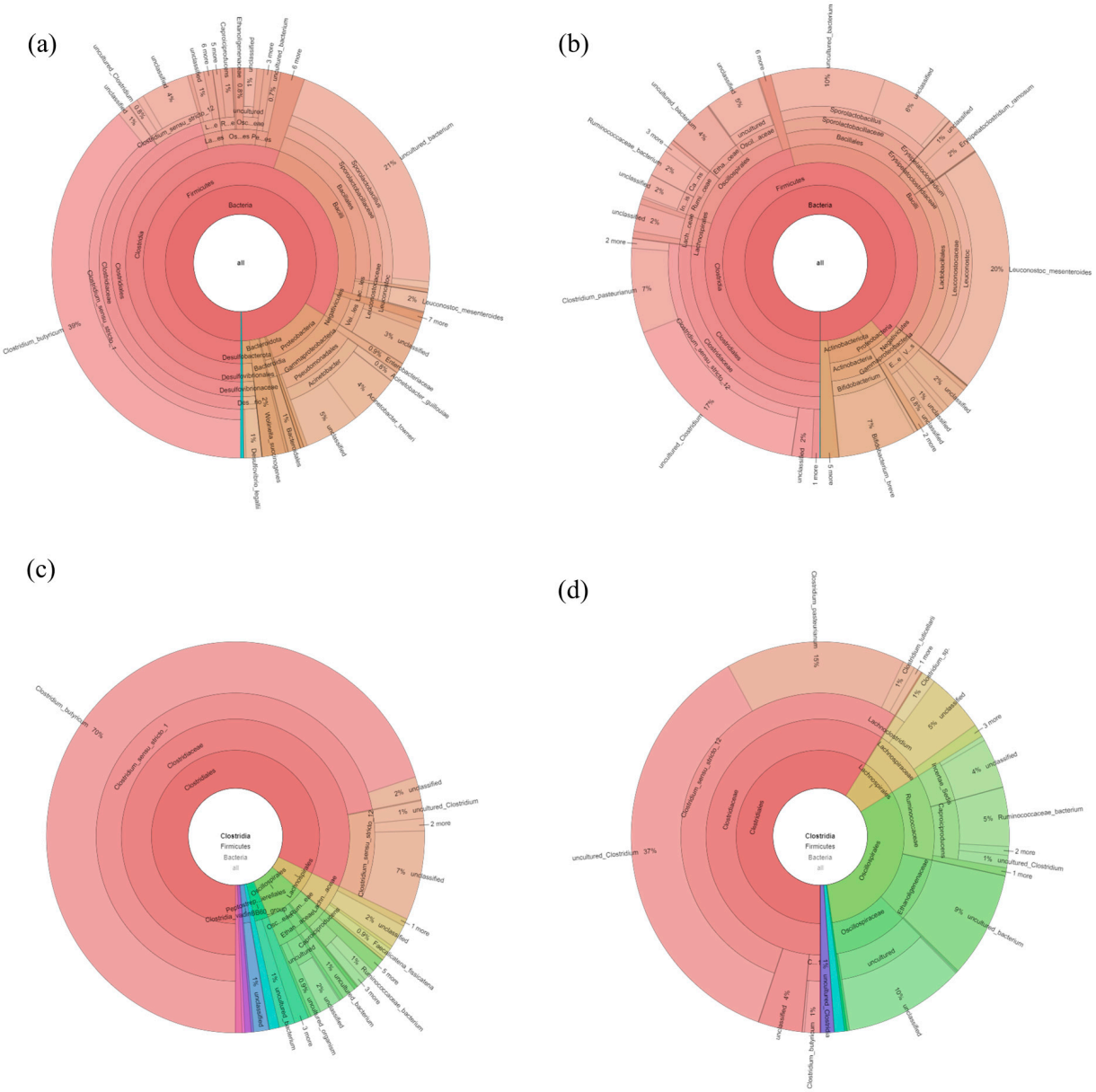


Figure 3. Microbial community composition: (**a**) before and (**b**) after continuous operation; internal taxonomic composition of the *Clostridia* fraction within the microbial community: (**c**) before and (**d**) after continuous operation.

3.4. Significances of the Experimental Data and Future Works

HPR and HY are two critical, distinct performance indicators in biohydrogen production. HPR measures the speed of production, emphasizing reactor capacity, and high HPR is desirable for industrial scalability because it allows for smaller and more efficient reactors. HY measures efficiency, indicating how effectively bacteria convert raw material into fuel, and high HY ensures minimal wastage of the raw material [37,38]. To evaluate the biohydrogen production performance of this pilot-scale system, we compared the present work with some reports using molasses substrates (Table 1). Most work was conducted using laboratory-scale systems and pilot-scale systems are limited, though a full-scale plant was reported [12]. Therefore, comparisons between different studies are mainly used to support engineering performance positioning and should not be regarded as direct comparisons under identical operating conditions. Moreover, Ren et al. [10] used a working volume of 1.48 m^3 in a anaerobic reactor to continuously produce biohydrogen from molasses at

12–24 h HRTs and obtained an HPR of 1.5–2.1 L/L-d, values smaller than those in the present work. Detman et al. [28] used a packed bed bioreactor to treat molasses, though this gave lower HPR values (1.8–2.6 L/L-d) than those in the present work, but showed that *Bacilli* played an important role in biohydrogen production efficiency, which agrees with the observations of the present work. Based on the above observations, the successful performance of the 60 L pilot-scale UASB bioreactor with a high HPR value would indicate the feasibility of scaling-up such a system for fermentative biohydrogen production.

Table 1. Comparison of pilot-scale and full-scale biohydrogen production from molasses substrates.

Reactor Type/Volume (L)	HRT (h)	HPR (L/L-d)	HY (L/g Sugar)	References
CSTR reactor/1480	12–24	1.5–2.1	0.10–0.13	[10]
Packed-bed reactor/30	6	1.8–2.6	–	[28]
CSTR (full-scale)/105	5.8	~2.5–3.0	–	[12]
UASB/60	8	3.64	0.07	This study

Other than HPR and HY, there are some parameters that are commonly used in elucidating biohydrogen performance. These parameters include pH, ORP, hydrogen concentration in produced gas, substrate conversion, and the distribution of liquid metabolites. Table 2 summarizes the operational parameters commonly used in elucidating biohydrogen production performance. Biohydrogen is an affordable green hydrogen and has garnered interest [30,39]. It can be applied to fuel cells for power generation and can blend with a biomethane, called biohythane, for higher combustion efficiency [9,40,41]. Moreover, using DF as the first stage of a two-stage anaerobic process could obtain more energy recovery [14,42]. The successful performance of the reactor provides another useful experience in implementing fermentative biohydrogen production technology. To achieve this purpose, further studies like techno-economic and life cycle analyses are helpful [43–45].

Table 2. Summary of operational parameters used in elucidating biohydrogen production performance.

Category	Parameters (Values Obtained)	Significances
Operational environment	pH (6.05) ORP (−444 mV)	Favoring H_2-producers Providing anaerobic environment
H_2 production	H_2 concentration (33.2%)	H_2 fraction in produced gas Speed of H_2 production
	HPR (3.64 L/L-d) HY (0.26 L H_2/g $COD_{removed}$) HY (0.07 L H_2/g total $sugar_{removed}$)	Conversion efficiency from substrate
Substrate conversion	Total sugar removal (88%) COD removal (13.4%)	Main source of H_2 Organics mainly converted into VFAs
Liquid metabolites	Ethanol (1150 mg/L) Ratio of butyrate/acetate (1.8) Butyrate (2300 mg/L)	Ethanol-type fermentation might present Show main metabolic pathway Dominant VFAs

In addition, as mentioned before in Section 3.2.2, Metabolites, ethanol in the present system may represent both a competing metabolic product and a possible secondary inhibitory factor, rather than a major inhibitor. One of the solutions to elucidate this problem is checking via microbial community analysis. However, because the microbial community was characterized only before and after continuous operation, the temporal relationship between ethanol accumulation and microbial community shifts could not be

directly determined in this study. Further work with time-resolved microbial monitoring is needed to clarify the role of ethanol in molasses-based DF.

4. Conclusions

The present work demonstrates the continuous operation of a 60 L pilot-scale UASB dark fermentation system for biohydrogen production from molasses. The reactor achieved an average HPR of 3.64 L H_2/L-d under the tested conditions. Total sugar and COD removal efficiencies were 88% and 13.4%, respectively, suggesting that total sugar may serve as a more appropriate process indicator than COD alone for evaluating substrate conversion in molasses-based biohydrogen production. In addition, the butyrate/acetate ratio of 1.8 indicated that butyrate-type fermentation was the dominant metabolic pathway. In addition, after continuous operation, *Firmicutes* remained the dominant phylum, while the relative abundance of *Bacilli* increased after acclimation. Meanwhile, the internal structure of *Clostridia* shifted from a single-dominant pattern to a more diverse consortium, suggesting that microbial diversification may help maintain stable reactor performance.

Author Contributions: Z.-T.L. and C.-Y.L. contributed to the study's conception, design and material preparation. Data collection and analysis were performed by Z.-T.L. The first draft of the manuscript was written by Z.-T.L., C.-Y.L. contributed to the funding, data analysis, supervision, review and re-editing. All authors have read and agreed to the published version of the manuscript.

Funding: The authors gratefully acknowledge financial support by National Council of Science and Technology, Taiwan (NSTC 114-2218-E-035-003).

Data Availability Statement: The original contributions presented in this study are included in the article. Further inquiries are available from the corresponding author.

Conflicts of Interest: The authors have no relevant financial or non-financial interests to disclose.

Abbreviations

ASVs	Amplicon sequence variants
COD	Chemical oxygen demand
CSTR	Completely stirred tank reactor
DF	Dark fermentation
HPR	Hydrogen production rate
HRT	Hydraulic retention time
HY	Hydrogen yield
ISR	Inoculum-to-substrate ratio
ORP	Oxidation-reduction potential
PCR	Polymerase chain reaction
SMPs	Soluble metabolite products
UASB	Up-flow anaerobic sludge blanket
VFAs	Volatile fatty acids
VS	Volatile solids

References

1. Alvarez, A.J.; Fuentes, K.L.; Arias, C.A.; Chaparro, T.R. Production of Hydrogen from Beverage Wastewater by Dark Fermentation in an Internal Circulation Reactor: Effect on pH and Hydraulic Retention Time. *Energy Convers. Manag. X* **2022**, *15*, 100232. [CrossRef]
2. Fang, H.H.P.; Zhang, T. *Anaerobic Technology*; Imperial College Press: London, UK, 2015.
3. IEA Bioenergy. Environmental Sustainability: Role of Waste and Residues in Bioenergy Supply. IEA Bioenergy Review 2022. Available online: https://www.ieabioenergyreview.org/environmental-sustainability/ (accessed on 15 March 2026).

4. Kim, J.K.; Nhat, L.; Chun, Y.N.; Kim, S.W. Hydrogen Production Conditions from Food Waste by Dark Fermentation with Clostridium Beijerinckii KCTC 1785. *Biotechnol. Bioprocess Eng.* **2008**, *13*, 499–504. [CrossRef]
5. Moussa, R.N.; Moussa, N.; Dionisi, D. Hydrogen Production from Biomass and Organic Waste Using Dark Fermentation: An Analysis of Literature Data on the Effect of Operating Parameters on Process Performance. *Processes* **2022**, *10*, 156. [CrossRef]
6. Lay, C.H.; Kuo, S.Y.; Sen, B.; Chen, C.C.; Chang, J.S.; Lin, C.Y. Fermentative Biohydrogen Production from Starch-Containing Textile Wastewater. *Int. J. Hydrogen Energy* **2012**, *37*, 2050–2057. [CrossRef]
7. Jarosz, Z.; Kapłan, M.; Klimek, K.; Anders, D.; Dybek, B.; Herkowiak, M.; Hołaj-Krzak, J.T.; Syrotyuk, S.; Korobka, S.; Syrotyuk, H.; et al. Evaluation of Biohydrogen Production Depending on the Substrate Used—Examples for the Development of Green Energy. *Energies* **2024**, *17*, 2524. [CrossRef]
8. Singh, D.; Sirini, P.; Lombardi, L. Green Hydrogen Production from Biogas or Landfill Gas by Steam Reforming or Dry Reforming: Specific Production and Energy Requirements. *Energies* **2025**, *18*, 2631. [CrossRef]
9. Abdul, P.M.; Lay, C.H.; Lin, C.Y.; Vo, T.P.; Chang, C.M. Anaerobic Biohythane Production in an Internal Two-Stage Bioreactor: Kitchen Waste Concentration Optimization. *Energies* **2025**, *18*, 1. [CrossRef]
10. Ren, N.; Li, J.; Li, B.; Wang, Y.; Liu, S. Biohydrogen Production from Molasses by Anaerobic Fermentation with a Pilot-Scale Bioreactor System. *Int. J. Hydrogen Energy* **2006**, *31*, 2147–2157. [CrossRef]
11. Lee, K.S.; Chen, S.L.; Lin, C.Y.; Chang, J.S. Converting Waste Molasses Liquor into Biohydrogen via Dark Fermentation Using a Continuous Bioreactor. *Int. J. Hydrogen Energy* **2021**, *46*, 16546–16554. [CrossRef]
12. Ren, N.Q.; Li, J.Z.; Ding, J.; Yan, X.F.; Li, N.; Zhang, N.; Xing, D.F.; Qin, Z.; Liu, Q.L.; Guo, W.Q.; et al. Biomanufacturing of Hydrogen from Waste Molasses: A Full-Scale Application. *Environ. Sci. Ecotechnol.* **2025**, *26*, 100568. [CrossRef]
13. Sustainability Report 2024. Available online: https://www.taisugar.com.tw/CSR/Movie_Index.aspx?p=24&n=11192 (accessed on 3 December 2024).
14. Sukphun, P.; Wongfaed, N.; Wongarmat, W.; Kongjan, P.; Chu, C.Y.; Sittijunda, S.; Reungsang, A. Pilot-Scale Development of a Semi-Continuous System for Biohythane Production Using Hydrothermally Pretreated Mixed Napier Grass and Microalgae. *Int. J. Hydrogen Energy* **2025**, *127*, 859–870. [CrossRef]
15. Zhang, Q.; Jiao, Y.; He, C.; Ruan, R.; Hu, J.; Ren, J.; Toniolo, S.; Jiang, D.; Lu, C.; Li, Y.; et al. Biological Fermentation Pilot-Scale Systems and Evaluation for Commercial Viability towards Sustainable Biohydrogen Production. *Nat. Commun.* **2024**, *15*, 4539. [CrossRef] [PubMed]
16. Yang, G.; Wang, J. Changes in Microbial Community Structure during Dark Fermentative Hydrogen Production. *Int. J. Hydrogen Energy* **2019**, *44*, 25542–25550. [CrossRef]
17. del Pilar Anzola-Rojas, M.; da Fonseca, S.G.; da Silva, C.C.; de Oliveira, V.M.; Zaiat, M. The Use of the Carbon/Nitrogen Ratio and Specific Organic Loading Rate as Tools for Improving Biohydrogen Production in Fixed-Bed Reactors. *Biotechnol. Rep.* **2015**, *5*, 46–54. [CrossRef]
18. American Public Health Association; Baird, R.; Eaton, A.D.; Rice, E.W.; Bridgewater, L.; American Water Works Association; Water Environment Federation. *Standard Methods for the Examination of Water and Wastewater*, 23rd ed.; American Public Health Association: Washington, DC, USA, 2017; ISBN 978-0-87553-287-5.
19. Laurentin, A.; Edwards, C.A. A Microtiter Modification of the Anthrone-Sulfuric Acid Colorimetric Assay for Glucose-Based Carbohydrates. *Anal. Biochem.* **2003**, *315*, 143–145. [CrossRef]
20. Chinnaraj, S.; Venkoba Rao, G. Implementation of an UASB Anaerobic Digester at Bagasse-Based Pulp and Paper Industry. *Biomass Bioenergy* **2006**, *30*, 273–277. [CrossRef]
21. Yu, S.; Sun, P.; Zheng, W.; Chen, L.; Zheng, X.; Han, J.; Yan, T. The Effect of COD Loading on the Granule-Based Enhanced Biological Phosphorus Removal System and the Recoverability. *Bioresour. Technol.* **2014**, *171*, 80–87. [CrossRef]
22. Lee, H.G.; Dulany, Z. Biogas and Hydrogen Production from Waste Biomass via Dark Fermentation Evaluating VFAs, COD, and HRT for Process Optimization. *Biomass* **2025**, *5*, 57. [CrossRef]
23. Chandra, R.; Bharagava, R.N.; Rai, V. Melanoidins as Major Colourant in Sugarcane Molasses Based Distillery Effluent and Its Degradation. *Bioresour. Technol.* **2008**, *99*, 4648–4660. [CrossRef]
24. Yang, M.; Ding, L.; Wang, P.; Wu, Y.; Areeprasert, C.; Wang, M.; Chen, X.; Wang, F.; Yu, G. Formation of Melanoidins and Development of Characterization Techniques during Thermal Pretreatment of Organic Solid Waste: A Critical Review. *Fuel* **2023**, *334*, 126790. [CrossRef]
25. Hastuti, Z.D.; Chu, C.Y.; Rachman, M.A.; Purwanto, W.W.; Dewi, E.L.; Lin, C.Y. Effect of Concentration on Biohydrogen Production in a Continuous Stirred Bioreactor Using Biofilm Induced Packed-Carrier. *Int. J. Hydrogen Energy* **2016**, *41*, 21649–21656. [CrossRef]
26. Vesga-Baron, A.; Etchebehere, C.; Schiappacasse, M.C.; Chamy, R.; Tapia-Venegas, E. Controlled Oxidation-Reduction Potential on Dark Fermentative Hydrogen Production from Glycerol: Impacts on Metabolic Pathways and Microbial Diversity of an Acidogenic Sludge. *Int. J. Hydrogen Energy* **2021**, *46*, 5074–5084. [CrossRef]
27. Fleitas García, A.-R.; Guez, J.-S.; Dussap, C.G.; Fontanille, P.; Christophe, G. Effect of Redox Potential on Biohydrogen Production during Dark Fermentation of Food Wastes in Bioreactor. *Int. J. Hydrogen Energy* **2025**, *141*, 1199–1210. [CrossRef]

28. Detman, A.; Laubitz, D.; Chojnacka, A.; Wiktorowska-Sowa, E.; Piotrowski, J.; Salamon, A.; Kaźmierczak, W.; Błaszczyk, M.K.; Barberan, A.; Chen, Y.; et al. Dynamics and Complexity of Dark Fermentation Microbial Communities Producing Hydrogen From Sugar Beet Molasses in Continuously Operating Packed Bed Reactors. *Front. Microbiol.* **2021**, *11*, 612344. [CrossRef]
29. Ghasemian, M.; Taheri, E.; Fatehizadeh, A.; Amin, M. Biological Hydrogen Production from Synthetic Wastewater by an Anaerobic Migrating Blanket Reactor: Artificial Neural Network (ANN) Modeling. *Environ. Health Eng. Manag.* **2019**, *6*, 269–276. [CrossRef]
30. Albuquerque, M.M.; Sartor, G.D.; Martinez-Burgos, W.J.; Scapini, T.; Edwiges, T.; Soccol, C.R.; Medeiros, A.B. Biohydrogen Produced via Dark Fermentation: A Review. *Methane* **2024**, *3*, 500–532. [CrossRef]
31. Karakaya, G.; Özmıhçı, S. Statistical Optimization of Biohydrogen Fermentation from a Perspective of Butyrate Production. *Int. J. Hydrogen Energy* **2024**, *67*, 807–817. [CrossRef]
32. Cappai, G.; De Gioannis, G.; Muntoni, A.; Spiga, D.; Boni, M.R.; Polettini, A.; Pomi, R.; Rossi, A. Biohydrogen Production from Food Waste: Influence of the Inoculum-To-Substrate Ratio. *Sustainability* **2018**, *10*, 4506. [CrossRef]
33. Wang, B.; Wan, W.; Wang, J. Inhibitory Effect of Ethanol, Acetic Acid, Propionic Acid and Butyric Acid on Fermentative Hydrogen Production. *Int. J. Hydrogen Energy* **2008**, *33*, 7013–7019. [CrossRef]
34. Ekwenna, E.B.; Tabraiz, S.; Wang, Y.; Roskilly, A. Exploring the Feasibility of Biological Hydrogen Production Using Seed Sludge Pretreated with Agro-Industrial Wastes. *Renew. Energy* **2023**, *215*, 118934. [CrossRef]
35. Silva-Martínez, R.D.; Aguilar-Juárez, O.; Díaz-Jiménez, L.; Valdez-Guzmán, B.E.; Aranda-Jaramillo, B.; Carlos-Hernández, S. Biological Hydrogen Production Through Dark Fermentation with High-Solids Content: An Alternative to Enhance Organic Residues Degradation in Co-Digestion with Sewage Sludge. *Fermentation* **2025**, *11*, 398. [CrossRef]
36. Correa-Villa, C.; Moreno-Cárdenas, E.; de Bruijn, J. Presence of Lactic Acid Bacteria in Hydrogen Production by Dark Fermentation: Competition or Synergy. *World J. Microb. Biotechnol.* **2024**, *40*, 380. [CrossRef] [PubMed]
37. Tomczak, W.; Ferrasse, J.-H.; Giudici-Orticoni, M.-T.; Soric, A. Effect of Hydraulic Retention Time on a Continuous Biohydrogen Production in a Packed Bed Biofilm Reactor with Recirculation Flow of the Liquid Phase. *Int. J. Hydrogen Energy* **2018**, *43*, 18883–18895. [CrossRef]
38. Martínez-Mendoza, L.J.; Muñoz, R.; García-Depraect, O. Continuous Fermentative Biohydrogen Production from Fruit-Vegetable Waste: A Parallel Approach to Assess Process Reproducibility. *Fermentation* **2025**, *11*, 545. [CrossRef]
39. European Biogas Association. Biohydrogen: Affordable, Green and Yet Overlooked. Available online: https://www.europeanbiogas.eu/biohydrogen-affordable-green-and-yet-overlooked/ (accessed on 15 March 2026).
40. Dimitriou, P.; Tsujimura, T. A Review of Hydrogen as a Compression Ignition Engine Fuel. *Int. J. Hydrogen Energy* **2017**, *42*, 24470–24486. [CrossRef]
41. Pandey, V.; Shahapurkar, K.H.; Guluwadi, S.; Mengesha, G.A.; Gadissa, B.; Banapurmath, N.R.; Vadlamudi, C.; Krishnappa, S.; Khan, T.M.Y. Studies on the Performance of Engines Powered with Hydrogen-Enriched Biogas. *Energies* **2023**, *16*, 4349. [CrossRef]
42. Li, J.; He, J.; Si, B.; Liu, Z.; Zhang, C.; Wang, Y.; Xing, X. A Pilot Study of Biohythane Production from Cornstalk via Two-Stage Anaerobic Fermentation. *Int. J. Hydrogen Energy* **2020**, *45*, 31719–31731. [CrossRef]
43. Alavi-Borazjani, S.A.; da Cruz Tarelho, L.A.; Capela, M.I. Biohythane Production via Anaerobic Digestion Process: Fundamentals, Scale-up Challenges, and Techno-Economic and Environmental Aspects. *Environ. Sci. Pollut. Res.* **2024**, *31*, 49935–49984. [CrossRef]
44. Jin, M.; Wei, X.; Mu, X.; Ren, W.; Zhang, S.; Tang, C.; Cao, W. Life-Cycle Analysis of Biohydrogen Production via Dark-Photo Fermentation from Wheat Straw. *Bioresour. Technol.* **2024**, *396*, 130429. [CrossRef]
45. Ganguly, A.; Sun, P.; Liu, X.; Delgado, H.E.; Sun, L.; Elgowainy, A. Techno-Economic and Life Cycle Analysis of Bio-Hydrogen Production Using Bio-Based Waste Streams through the Integration of Dark Fermentation and Microbial Electrolysis. *Green Chem.* **2025**, *27*, 6213–6231. [CrossRef]

Disclaimer/Publisher's Note: The statements, opinions and data contained in all publications are solely those of the individual author(s) and contributor(s) and not of MDPI and/or the editor(s). MDPI and/or the editor(s) disclaim responsibility for any injury to people or property resulting from any ideas, methods, instructions or products referred to in the content.